Separation and Purification Technology 329 (2024) 125159

Contents lists available at ScienceDirect

Separation and Purification Technology

journal homepage: www.elsevier.com/locate/seppur

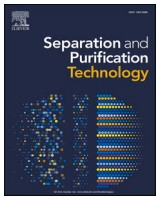

Effective removal and recovery of phosphorus using ZnAl-COOH-modified biochar via hydrogen bonds

Yimin Huang [a,b], Dafeng Zhang [c], Hongguang Cheng [a,*], Yingnan He [d], Guangzhi Hu [d,*]

[a] State Key Laboratory of Environmental Geochemistry, Institute of Geochemistry, Chinese Academy of Science, Guiyang, Guizhou 550081, China
[b] Faculty of Environmental Science and Engineering, Kunming University of Science and Technology, Kunming 650504, China
[c] School of Materials Science and Engineering, Liaocheng University, Liaocheng 252000, China
[d] Institute for Ecological Research and Pollution Control of Plateau Lakes, School of Ecology and Environmental Science, Yunnan University, Kunming 650504, China

ARTICLE INFO

Keywords:
Carboxylated biochar
Hydrogen bonds
Selective adsorption
Phosphorus recovery

ABSTRACT

The global community is facing the dual problem of water eutrophication and a shortage of phosphate rock resources. In this study, carboxylated ZnAl-hydroxide-modified biochar (LDH/PMA/BC) was synthesised to remove and recover phosphorus (P) from water through highly selective adsorption and desorption of P. The results of adsorption experiments indicated that LDH/PMA/BC has an high removal rate for low concentrations of P, and the maximum capacity for adsorption of P was 109 mg g^{-1}. Furthermore, when a low concentration of P coexisted with a high concentration of competitive ions, LDH/PMA/BC could selectively adsorb P through hydrogen bonding, and its removal rate for P reached 99 %–100 % of its removal rate without competitive ions. In addition, LDH/PMA/BC maintained 85 %–93 % of its initial adsorption capacity in 10 adsorption–desorption cycles, and the P recovery rate reached 95 %. These results indicate the potential of LDH/PMA/BC as an adsorbent for removing and recovering P from wastewater.

1. Introduction

Water eutrophication is one of the environmental problems that urgently needs to be solved globally. P is the main element that causes the eutrophication of water bodies [1]. However, it is also one of the essential nutrients in ecosystems. Currently, phosphate rock is the primary source of industrial phosphate production [2]. With the increase in the global population, the demand for phosphate rock in industry, e.g. agriculture, is increasing exponentially, and phosphate rock will be depleted within the next 50–100 years [3,4]. In addition, the increased use of P has caused increasing amounts of P to enter the water system through secondary pollution, such as industrial, city, and agricultural runoff and sewage sludge, of which approximately 80 % is discharged with sewage [5,6]. Therefore, developing technologies for recovering high-purity P from P-containing wastewater is the key to controlling P pollution and resolving the shortage of phosphate rock resources [7,8].

The previously reported methods for treating P pollution in wastewater mainly include biological processes, chemical precipitation, ion exchange, and adsorption [9]. Among these methods, the adsorption method has the advantages of low energy consumption, easy operation, and P recovery through desorption [6,10]. Therefore, it has broad application prospects in removing and recovering P from wastewater [11]. The primary forms of P in water are $H_2PO_4^-$ and HPO_4^{2-}, and common anions coexisting with P include Cl^-, SO_4^{2-}, CO_3^{2-}, HCO_3^-, and NO_3^-. Because these anions and P have similar chemical properties, the anions can compete with P, reducing the adsorption capacity of the adsorbent [12]. Therefore, the key to solving the problem of P pollution through adsorption is to develop an adsorbent with a highly adsorption capacity and selectivity to P and solve the problem of adsorption competition between coexisting anions and P [13]. The selectivity of an adsorbent towards P is determined by its adsorption mechanism. From a thermodynamic viewpoint, if the adsorbent has a high selectivity for adsorbing P, it has formed a strong chemical bond with P [14], which makes P desorption difficult. For example, lanthanum oxide (hydroxide) has a highly selective adsorption capacity because lanthanum can form a strong bond with P ($LaPO_{4(s)}$). However, desorbing P from the surface of lanthanum oxide (hydroxide) is challenging [15], as confirmed by our previous research [9].

The development of adsorbents based on hydrogen bonding is a possible way to achieve highly selective adsorption and recovery of P [16]. The primary forms of P in sewage ($H_2PO_4^-$ and HPO_4^{2-}) contain -H and can function as hydrogen-bond donors. However, common ions

* Corresponding authors.
E-mail addresses: chenghongguang@vip.gyig.ac.cn (H. Cheng), guangzhihu@ynu.edu.cn (G. Hu).

https://doi.org/10.1016/j.seppur.2023.125159
Received 28 March 2023; Received in revised form 5 September 2023; Accepted 19 September 2023
Available online 21 September 2023

coexisting with P, such as Cl^-, SO_4^{2-}, NO_3^-, and CO_3^{2-}, exist in a deprotonated state and can only be hydrogen-bond receptors. Hence, if the adsorbent contains hydrogen-bond acceptor groups, it can form hydrogen bonds with hydrogen-bond donors $H_2PO_4^-$ and HPO_4^{2-} without being affected by Cl^-, SO_4^{2-}, NO_3^-, and CO_3^{2-}. In addition, hydrogen bonds are easily destroyed; therefore, P adsorbed by a hydrogen bond is easily desorbed [12], which is conducive to P recovery and adsorbent regeneration. A few relevant studies have partially indicated the effectiveness of this method. For example, Saha et al. [17] modified alkaline Al_2O_3 with 1,3,5-benzenetricarboxylic acid ($C_9H_6O_6$). The carboxylated Al_2O_3 selectively adsorbed 90 % of H_3PO_4 from an H_3PO_4 solution containing Cl^-, NO_3^-, and Br^-, and 100 % of the adsorbed P was desorbed from the surface of carboxylated Al_2O_3.

Although the above research preliminarily confirmed that the adsorbent's adsorption of P based on hydrogen bonding avoids the competition of many coexisting ions (Cl^-, SO_4^{2-}, NO_3^-, and CO_3^{2-}), some anions can be hydrogen-bond donors, competing with $H_2PO_4^-$ and HPO_4^{2-}. HCO_3^- is a representative hydrogen-bond donor that is found in high concentrations in sewage. When HCO_3^- coexists with $H_2PO_4^-$ and HPO_4^{2-}, it is unclear which preferentially forms hydrogen bonds with the hydrogen-bond receptor functional group on the adsorbent. In addition, the concentration of HCO_3^- in actual wastewater is frequently several times higher than that of $H_2PO_4^-$ and HPO_4^{2-}; however, the effect of such a significant concentration difference on the ability of the adsorbent to selectively adsorb P is unclear. In addition, owing to the limited research on the adsorption of P via hydrogen bonding, the improvement of the adsorption capacity of the adsorbent based on hydrogen bonding to adsorb P is worthy of further research.

In this study, we intended to use the carboxyl groups on pyromellitic acid (PMA) as hydrogen bonding acceptors to form hydrogen bonds with P; however, PMA is unstable in an aqueous solution and hence, is not suitable for use as an adsorbent. Therefore, we prepared stable adsorbents (LDH/PMA) by intercalating PMA into the interlayer of Zn-Al-LDH through anion exchange. Moreover, to increase the number of exposed adsorption sites on LDH/PMA and facilitate separation from water, we doped LDH/PMA with wheat straw biochar (BC). The final synthesized sample is named LDH/PMA/BC. (LDH is a Zn-Al layered double hydroxide, and LDH/PMA is a Zn-Al layered double hydroxide with PMA inserted). The adsorption mechanism of LDH/PMA/BC for P was investigated via characterisation of the surface functional groups of the adsorbent, adsorption kinetics, isotherms, and a thermodynamic analysis. In addition, the effects of the type (hydrogen-bond acceptor or hydrogen-bond donor) and concentration of competitive ions on the selectivity of LDH/PMA/BC to P were investigated. These insights can contribute to the development of novel strategies for highly selective P removal and recovery.

2. Materials and methods

2.1. Materials and reagents

Wheat straw was obtained from a farm in Yunnan Province, China. Pyromellitic dianhydride (PMDA; $C_{10}H_2O_6$), zinc chloride ($ZnCl_2$), and aluminium chloride hexahydrate ($AlCl_3{\cdot}6H_2O$) were obtained from Aladdin Reagent Company, China. Hydrochloric acid (HCl) was purchased from Kelon Chemical Reagent Co., Chengdu, China. Sodium hydroxide (NaOH) was purchased from Tianjin Fengchuan Chemical Reagent Technology Co., Ltd., China. All reagents were used as received, without further purification.

2.2. Synthesis of adsorbents

2.2.1. Preparation of biochar

Wheat straw was dried and ground into powder. An NaOH solution (45 mL, 2 M) was poured into a plastic beaker containing wheat straw powder (21 g), and placed in a tubular furnace. N_2 was continuously injected into the tubular furnace to prevent biochar from being oxidised, and the temperature was increased to 800 °C at a rate of 10 °C min^{-1}. The heating was turned off after the temperature was maintained at 800 °C for 2 h. The tubular furnace was naturally cooled to 25 °C, and the obtained samples were denoted as BC. Next, BC was added to ultrapure water (500 mL), the pH of the suspension was adjusted to 7 with HCl, and the suspension was stirred for 12 h at room temperature. Then, the BC was washed and filtered until the pH of the filtrate was natural. Finally, the BC was dried at 60 °C.

2.2.2. Preparation of adsorbents

First, BC (1.5 g), $ZnCl_2$ (14.061 g), and $AlCl_3{\cdot}6H_2O$ (12.45 g) were added to a beaker containing ultrapure water (300mL), and the mixture was stirred for 12 h at 25 °C (named A_1 solution). Second, PMDA (11.25 g) was added to another beaker containing ultrapure water (90 mL), the pH of the solution was adjusted to 12 using the NaOH solution (2 M), and the mixture was stirred until PMDA was completely dissolved (named A_2 solution). Third, the A_1 solution was poured into the beaker containing the A_2 solution, and the pH of the mixed solution (A_1 + A_2) was adjusted to 10 with the NaOH solution (2 M).

Then, the mixture was stirred for 1 h at 25 °C. The beaker containing the mixture was placed in an oven set to 65 °C [2]. Fourth, after 12 h, the beaker was removed from the oven and cooled to room temperature. Then, the suspension in the beaker was filtered and washed until the pH of the filtrate was 7. Finally, the solid sample was dried at 70 °C for 24 h and grounded for standby. The sample with the layered double hydroxyl structure was named LDH/PMA/BC. As the control sample, LDH and LDH/PMA were synthesised using the above method. The reason why the sample was so named is that PMDA is first hydrolysed into phthalic acid (PMA) in the aqueous solution, and then PMA is intercalated between the LDH layers through anion exchange with LDH. Therefore, the LDH modified by PMDA was named LDH/PMA, and the BC modified with LDH/PMA was named LDH/PMA/BC. In addition, to study the influence of the weight proportion of BC in LDH/PMA/BC on the adsorption effect of LDH/PMA/BC, LDH/PMA/BC containing with different weights ratios of biochar were synthesised. For BC:PMDA weight ratios (g:g) of 0.5:1, 0.33:1, 0.17:1, 0.125:1, and 0.1:1, the synthesised samples were named LDH/PMA/BC_1, LDH/PMA/BC_2, LDH/PMA/BC_3, LDH/PMA/BC, and LDH/PMA/BC_4, respectively (Fig. 1).

2.3. Adsorbent characterisation

The surface characteristics, surface functional groups, surface element composition, and pore diameter and specific surface area of the adsorbent were analysed using scanning electron microscopy (SEM; Zeiss Sigma300, Germany), Fourier-transform infrared (FTIR) spectroscopy (Bruker MPA and Tensor 27, Germany), X-ray photoelectron spectroscopy (XPS; Thermo Fisher K-Alpha+, USA), and a specific surface area and porosity analyser (Brunauer–Emmett–Teller (BET); TriStar II 3Flex, USA), respectively. In addition, the X-ray diffraction (XRD) patterns of the samples were collected using an X-ray diffractometer (Rigaku Ultima IV, Japan).

2.4. Adsorption experiments

For all the adsorption experiments performed in this study, the conditions were set as follows: the ratio of adsorbent to P solution was 0.4:1 (g:L), the reaction temperature was 25 °C, and the pH of the solution was 7. Each experiment was performed three times. The differences in the experimental conditions from those above are described in the following scheme.

Adsorption experiments without competitive ions: 1) The effect of the solution pH on the adsorption capacities of different adsorbents was investigated. The specific experimental conditions were as follows: the pH of the P solution with an initial concentration of 100 mg/L was adjusted to 3.0, 4.0, 5.0, 6.0, 7.0, and 8.0 using NaOH and HCl with a

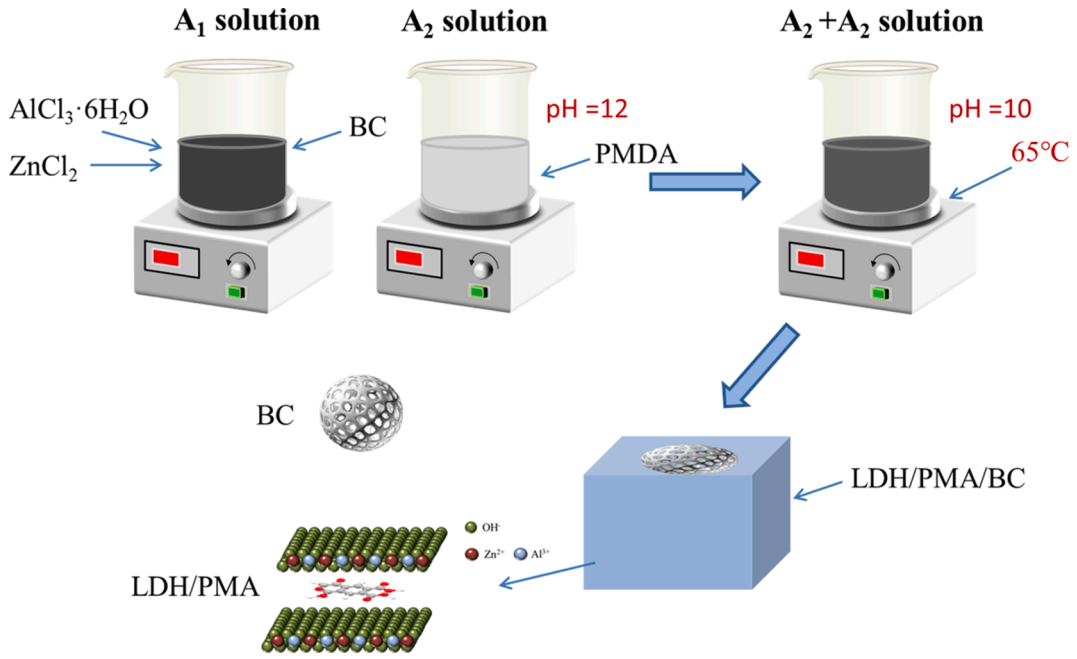

Fig. 1. Flowchart of LDH/PMA/BC preparation.

concentration of 0.1 M. 2) Isothermal adsorption curves were investigated at three temperatures (10, 25, and 40 °C), and the initial concentration of the P solution was 10, 20, 50, 100, and 200 mg/L. 3) The adsorption kinetics were also studied. Specifically, the adsorption capacity of the adsorbent at different adsorption times for P with initial concentrations of 20 and 100 mg/L was evaluated.

Adsorption experiments with competitive ions: 1) six experiments were conducted, and the initial P concentration of the solution was 0.0004 mol/L. The initial concentration of competitive ions (Cl^-, SO_4^{2-}, and NO_3^-) in each experiment was the same, and the concentrations of competitive ions in the six experiments were 0.0004, 0.002, 0.004, 0.02, and 0.04 mol/L. 2) Three experiments were conducted; the initial P concentration of the solution was 0.0004 mol/L, and the concentrations of competitive ions (HCO_3^-) in the three experiments were 0.0004, 0.002, and 0.004 mol/L.

After the adsorption reached equilibrium, a 0.45-μm microporous membrane was used to filter the suspension. An ultraviolet spectrophotometer was used to determine the content of P in the filtrate; anion chromatography was used to determine the contents of Cl^-, SO_4^{2-}, and NO_3^- in the filtrate; and the CO_3^{2-} and HCO_3^- in the filtrate were titrated using double-indicator titration.

The adsorption capacity of the adsorbent for various anions is calculated as equation S1[7]. The capacity of the adsorbent to selectively adsorb P is calculated as equation S2. The dynamic parameters are fitted by the pseudo-first- and pseudo-second-order models (equation S3 and S4) [18]. The isothermal adsorption data fitted by the Langmuir equation[19] and the Freundlich equation[20] (equation S5 and S6). The separation factor (R_L) is calculated as equation S7 [21].

2.5. Desorption experiment

After the adsorption experiment, the sample was transferred to a centrifuge tube. It was centrifuged, and the supernatant was removed from the centrifuge tube. Then, an NaOH desorption solution with a concentration of 0.1 mol/L (20 mL) was injected into the centrifuge tube, and the tube was shaken for 4 h. Finally, the sample was centrifuged again, and the supernatant was extracted and filtered to measure the concentration of P.

3. Results and discussion

3.1. Sample characterisation

3.1.1. SEM and BET analysis

The surface characteristics of LDH, LDH/PMA, and LDH/PMA/BC were compared (Fig. S1). SEM analysis of three adsorbents in support materials. SEM images indicated that the addition of BC resulted in the appearance of abundant pores on the surface of LDH/PMA. Therefore, we compared the specific surface area and pore volume of BC, LDH, LDH/PMA, and LDH/PMA/BC (Fig. 2b). BC had a large specific surface area (458.7 m^2/g) and abundant pores (pore volume of 0.25 $cm^3\ g^{-1}$). The specific surface area and pore volume of LDH were small (1.8 m^2/g, 0.002 $cm^3\ g^{-1}$). The specific surface area of LDH modified by PMA was only 2.1 m^2/g, and its pore volume was only 0.004 $cm^3\ g^{-1}$. When BC was doped onto LDH/PMA, its specific surface area increased by a factor of 20 to 47.3 m^2/g, and its pore volume increased to 0.02 $cm^3\ g^{-1}$. The abundant pores on the surface of LDH/PMA/BC increased the number of surface functional groups exposed, slightly increasing its adsorption capacity for P.

3.1.2. XRD analysis

The XRD analysis results of LDH, LDH/PMA, and LDH/PMA/BC were compared (Fig. 2a). For LDH, a characteristic peak representing the (0 0 3) reflection of the LDHs appeared at 11.59°, confirming that the synthesised LDH had a layered structure. In addition, the peaks at 2θ values of approximately 21°, 34°, 39°, 46°, and 61° corresponded to the (0 0 6), (0 1 2), (0 1 5), (0 1 8), and (1 1 0) reflections of the LDHs (Fig. 2a). These peaks indicated the formation of crystalline phases of LDHs [22].

With the insertion of PMA, the (0 0 3) characteristic peak shifted from 11.234° to 10.124°, and the basal spacing expanded from 0.787 to 0.873 nm (Fig. 2a). The basal-spacing value of PMA-LDH (0.873 nm) minus the thickness of the main layer of LDH (0.48 nm) [2] is the gallery height value of PMA-LDH (0.393 nm). The gallery height value of PMA-LDH determines how PMA is inserted into LDH. Considering that the size of PMA is 0.70 nm × 0.53 nm × 0.21 nm [23], this result confirms that PMA is intercalated into the LDHs with a horizontal orientation. After BC was loaded onto PMA-LDH (named PMA/LDH/BC), the position of the characteristic peak (0 0 3) did not shift, indicating that biochar does not

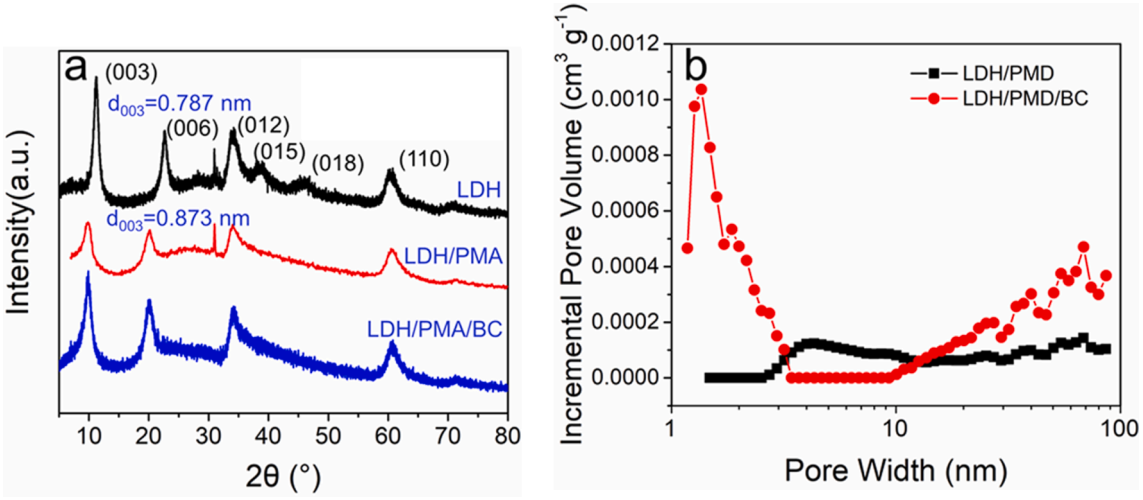

Fig. 2. (a) XRD analysis results for LDH, LDH/PMA, and LDH/PMA/BC. (b) Pore size and pore volume distributions of LDH, LDH/PMA, and LDH/PMA/BC.

affect the intercalation of PMA into LDH.

3.1.3. FTIR analysis

To compare the functional groups of BC, LDH, LDH/PMA, and LDH/PMA/BC, we compared and analysed their FTIR spectra (Fig. 3a). For the surface of BC, there were three peaks at 3450.2, 1572.4, and 1128.1 cm^{-1}, which corresponded to –OH, C/C = O, and C-O, respectively [24]. LDH exhibited a broad band at 3458.1 cm^{-1} representing the metal-OH

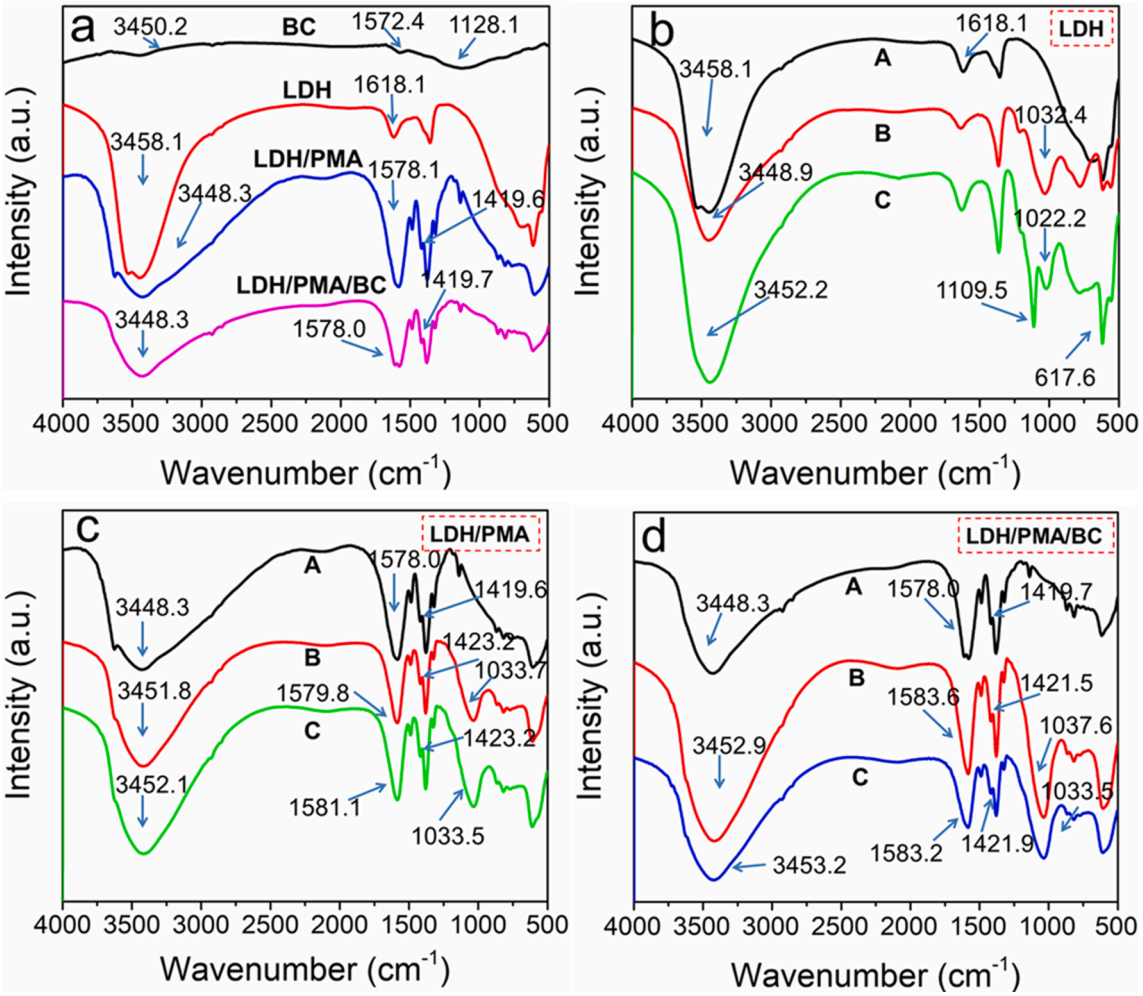

Fig. 3. (a) FTIR spectra of BC, LDH, LDH/PMA, and LDH/PMA/BC. (b) FTIR spectra of LDH before and after adsorption. (c) FTIR spectra of LDH/PMA before and after adsorption. (d) FTIR spectra of LDH/PMA/BC before and after adsorption. (Curves A, B, and C represent the spectra before adsorption, after adsorption of P, and after adsorption of P and coexisting ions, respectively.).

stretching, indicating the abundance of –OH in the LDH structure. Another weak peak for LDH at 1618.1 cm^{-1} corresponded to the bending vibration of adsorbed H_2O [22]. When PMA was inserted into LDH (named LDH/PMA), the peak of LDH at 3458.1 cm^{-1} shifted to 3448.3 cm^{-1}, and the width of the peak increased. This is because the PMA introduced rich –COOH, and the wide peak at 3448.3 cm^{-1} represented the –OH of carboxylic acid. In addition, LDH/PMA exhibited antisymmetric and symmetric stretching peaks attributed to $–COO^-$ at 1578.1 and 1419.6 cm^{-1}, respectively. The changes in these peaks confirmed that PMA was successfully inserted into LDH. Notably, the characteristic peak of LDH/PMA/BC was consistent with the characteristic peak of LDH/PMA, indicating that the BC did not change the functional groups of LDH/PMA. The reason why the BC did not affect the functional groups of LDH was that the biochar carbonised at 800 °C mainly had a C structure, and it had few O-containing functional groups; thus, the influence of BC on the functional groups of LDH/PMA was small.

To explore the adsorption mechanisms of LDH, LDH/PMA, and LDH/PMA/BC, we analysed the FTIR spectra of LDH, LDH/PMA, and LDH/PMA/BC before P adsorption (curve A in Fig. 3b, 3c, and 3e), after P adsorption (curve B Fig. 3b, 3c, and 3e), and after the adsorption of P and coexisting ions (curve C in Fig. 3b, 3c, and 3e). As shown in Fig. 3b, for LDH, when the solution only contained P, a peak representing P = O appeared at 1032.4 cm^{-1} [25], confirming that P was successfully adsorbed on the surface of LDH. Meanwhile, the peak corresponding to the stretching vibration of the –OH group in LDH was shifted from 3458.1 to 3448.9 cm^{-1}, suggesting that the –OH group participated in the P adsorption, which indicated that LDH mainly adsorbed P through the mechanism of ligand exchange. When the solution contained P and coexisting ions, the peak of LDH representing P = O at 1032.4 cm^{-1} was shifted to 1022.2 cm^{-1}, and a new peak representing adsorbed coexisting anions appeared at 1109.5 cm^{-1}, indicating that LDH can adsorb not only P but also coexisting ions, with low selectivity for P. This is consistent with the results of the adsorption experiment presented in Section 3.2 (see Fig. 5c).

For LDH/PMA (Fig. 3c), when the solution only contained P, a significant peak representing P = O appeared at 1033.7 cm^{-1}. Meanwhile, the peak of –OH from carboxylic acid and the antisymmetric and symmetric stretching peaks of $–COO^-$ were shifted to 3376, 1578, and 1418 cm^{-1}, respectively. This proves that P was successfully adsorbed on LDH/PMA and that the carboxyl group on LDH/PMA was the main functional group for adsorbing P through the formation of hydrogen bonds. Therefore, the main mechanism of LDH/PMA adsorption of P is hydrogen bonding. When the solution contained P and coexisting ions, a peak representing P = O was observed for the surface of LDH/PMA at 1033.5 cm^{-1}, but no new peak representing adsorbed coexisting ions appeared for the surface of LDH/PMA, in contrast to the results for LDH. This phenomenon indicated that even when P exists together with coexisting ions, LDH/PMA only selectively adsorbs P via hydrogen bonding.

For LDH/PMA/BC (Fig. 3d), when the solution only contained P, a significant peak representing P = O also appeared at 1037.6 cm^{-1}. Meanwhile, the peaks representing carboxyl groups at 3448.3, 1578.0, and 1419.7 cm^{-1} were shifted to 3452.9, 1583.6, and 1421.5 cm^{-1}, respectively. This phenomenon is consistent with the phenomenon after LDH/PMA adsorbs P and also proves that LDH/PMA/BC adsorbs P through the formation of hydrogen bonds between carboxyl groups and P. When the solution contained P and coexisting ions, LDH/PMA only exhibited a peak representing P = O (1033.5 cm^{-1}); there was no new peak representing the adsorbed coexisting ions as in the case of LDH, indicating that even when P is combined with coexisting ions, PMA only selectively adsorbs P through hydrogen bonding.

3.1.4. XPS analysis

To further investigate the P adsorption mechanism of LDH, LSH/PMA, and LDH/PMA/BC, XPS was conducted (Fig. 4). First, we analysed the XPS spectra of LDH before adsorption of P, after adsorption of P, and after adsorption of P and coexisting anions (Fig. 4a, 4d, 4 g, and 4 m). After adsorption of P (the solution only contained P), a peak corresponding to P 2p appeared for the surface of LDH (Fig. 4m), indicating that P was successfully adsorbed. The P 2p peak was deconvoluted into three peaks at 131.3 and 132.1 eV, corresponding to HPO_4^{2-} and $H_2PO_4^-$, respectively [26]. Meanwhile, the peaks representing Zn 2p, Al 2p, and O 1 s in LDH exhibited significant shifts. Specifically, the Zn 2p peaks shifted from 1044.4 and 1021.3 eV to 1043.6 and 1020.6 eV (Fig. 4a), the Al 2p peak shifted from 74.6 to 73.1 eV (Fig. 4d), and the O 1 s peak shifted from 531.4 to 530.4 eV (Fig. 4g). One of the reason for the significant shifts of these three peaks was the ligand exchange between P and –OH on LDH, which resulted in the formation of an inner sphere complex between P and Zn/Al on LDH, as reported by Zhang [26]. Another reason is that the interlayer anions in LDH exchange with P. When there were P and coexisting ions in the solution, the shifts of the Zn 2p, Al 2p, and O 1 s peaks of LDH after adsorption were insignificant, indicating that the presence of coexisting ions did not affect the adsorption mechanism of LDH for P. Therefore, the main adsorption mechanism of LDH for P/coexisting ions is the ligand exchange between P/coexisting ions and –OH, as well as the ion exchange between interlayer ions of LDH and P/coexisting ions.

Compared with LDH, the Al 2p peak of LDH/PMA was not changed after P adsorption, although the Zn 2p and O 1 s peaks exhibited slight shifts (Fig. 4b, 4e, 4 h, 4j, and 4n). Specifically, the peaks of Zn 2p shifted from 1043.5 and 1020.5 eV to 1043.6 and 1020.6 eV (Fig. 4b), and the peak of O 1 s shifted from 530.3 to 530.4 eV (Fig. 4h). The significant differences in the peaks between LDH/PMA and LDH after P adsorption indicated that the LDH/PMA and LDH had different P adsorption mechanisms. To further investigate the adsorption mechanism of LDH/PMA for P, we analysed the changes in the C1s peak of LDH/PMA after P adsorption (Fig. 4j). The C 1 s XPS spectrum of LDH/PMA can be deconvoluted into two peaks at 286.7 and 282.9 eV, corresponding to $–COO^-$ [26], C–C, and C–H in the aromatic ring of PMA [2]. After the adsorption of P, the binding energy of the COO^- peak was reduced from 286.7 to 286.4 eV because the -C = O and –OH on carboxylic acid formed one or two hydrogen bonds with the -P-OH and -P-O on phosphate [26]. Therefore, hydrogen bonding is the main adsorption mechanism of LDH/PMA for P. When P coexisted with ions in the solution, the binding energies of the Zn 2p, Al 2p, O 1 s, and C 1 s peaks for LDH/PMA were almost identical to those when LDH/PMA only adsorbed P, with only slight shifts of the Zn 2p and Al 2p peaks. This result indicated that LDH/PMA mainly adsorbs P through hydrogen bonding and only adsorbs a small amount of coexisting ions by forming the inner sphere complex with Zn/Al on LDH/PMA/BC; thus, LDH/PMA has high selectivity for P.

For LDH/PMA/BC, after the adsorption of P or P and coexisting ions (the solution contained either P alone or P and coexisting ions), the shifts of the Zn 2p, Al 2p, O 1 s, and C 1 s peaks for LDH/PMA/BC were consistent with the shifts of the Zn 2p, Al 2p, O 1 s, and C 1 s peaks for LDH/PMA (Fig. 4c, 4f, 4i, 4 k, 4 l and 4o), indicating that the addition of BC did not alter the adsorption mechanism of LDH/PMA for P. Thus, LDH/PMA/BC still adsorbed P through hydrogen bonding, LDH/PMA/BC still adsorbed P through hydrogen bonding, and high selectivity for P was maintained, which was consistent with the results of the adsorption experiment presented in Section 3.2 (Fig. 5c).

3.2. Comparison of adsorption capacities of different adsorbents

To investigate the roles of Zn/Al (LDH), PMA, and BC in the P adsorption process of LDH/PMA/BC, the influence of the proportion of BC in LDH/PMA/BC on the P adsorption capacity of LDH/PMA/BC was first investigated (Fig. 5b). The reason is that BC cannot adsorb P; however, the doping concentration of BC affects the proportion of LDH/PMA in LDH/PMA/BC and thus, leads to a change in the P adsorption properties of LDF/PMA/BC. In this study, the proportions (g:g) of BC and

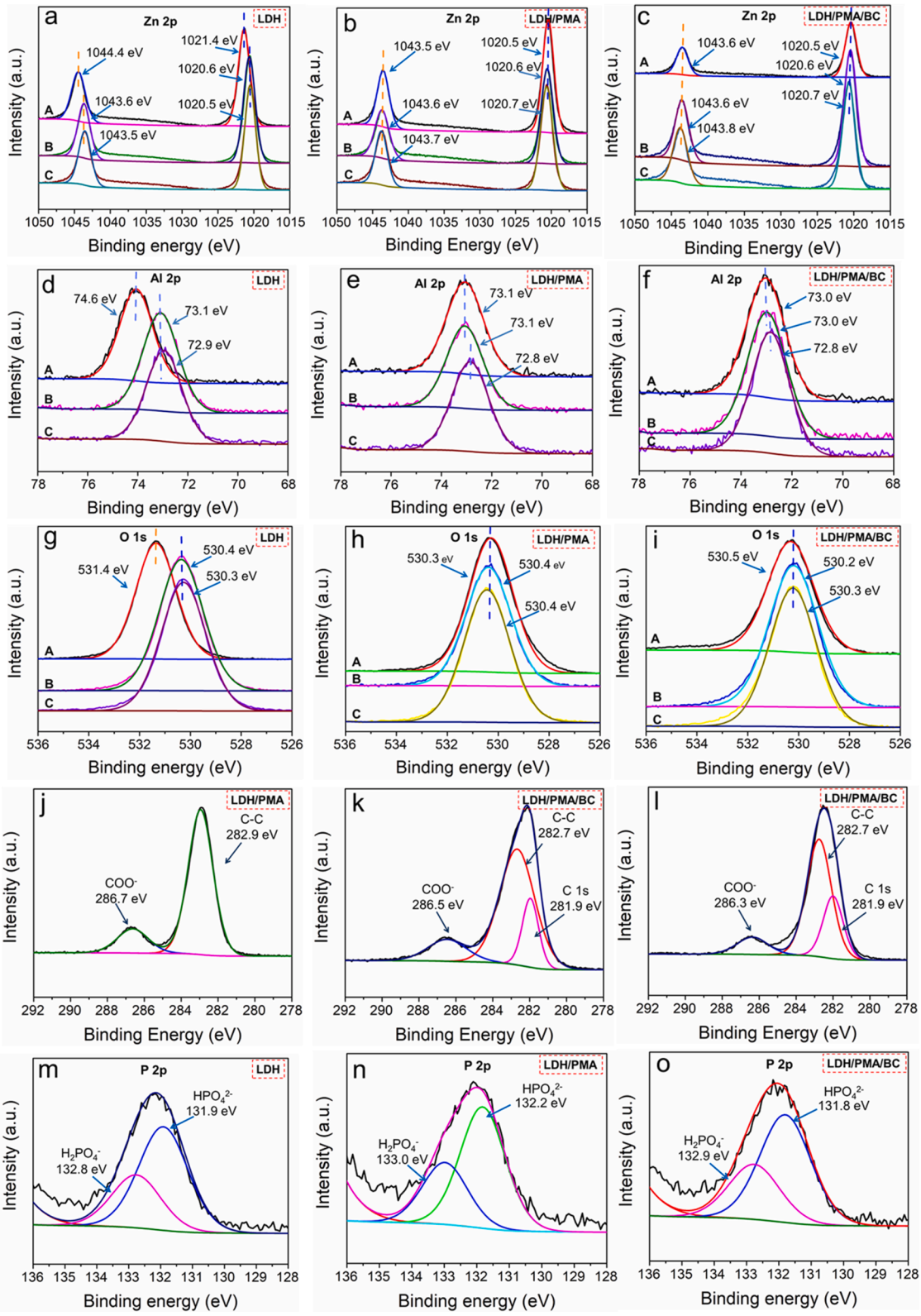

Fig. 4. XPS analysis results for LDH, LDH/PMA, and LDH/PMA/BC. (a) Zn 2p spectra of LDH before and after adsorption; (b) Zn 2p spectra of LDH/PMA before and after adsorption; (c) Zn 2p spectra of LDH/PMA/BC before and after adsorption. (d) Al 2p spectra of LDH before and after adsorption; (e) Al 2p spectra of LDH/PMA before and after adsorption; (f) Al 2p spectra of LDH/PMA/BC before and after adsorption. (g) O 1 s spectra of LDH before and after adsorption; (h) O 1 s spectra of LDH/PMA before and after adsorption; (i) O 1 s spectra of LDH/PMA/BC before and after adsorption. (j) C 1 s spectrum of LDH/PMA; C 1 s spectra of LDH/PMA/BC (k) before and (l) after adsorption. (m) P 2p spectrum of P-adsorbed LDH/PMA/BC. (n) P 2p spectrum of P-adsorbed LDH/PMA/BC. (o) P 2p spectrum of P-adsorbed LDH/PMA/BC. (Curves A, B, and C represent the spectra before adsorption, after adsorption of P, and after adsorption of P and coexisting ions, respectively.).

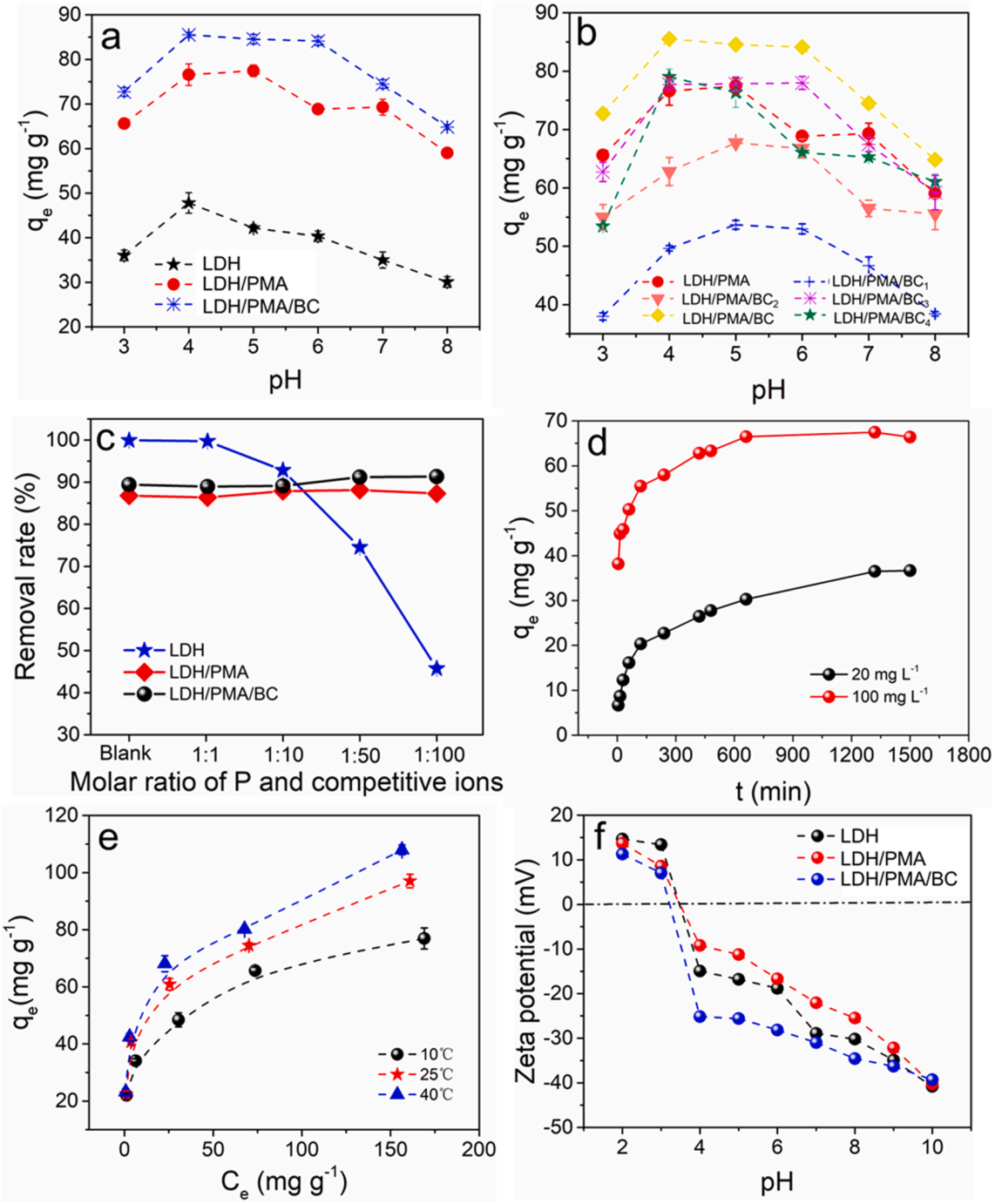

Fig. 5. (a) Effect of the pH on the adsorption capacities of LDH, LDH/PMA, and LDH/PMA/BC. (b) Effect of the proportion of BC in LDH/PMA/BC on the adsorption capacity of LDH/PMA/BC. (c) Effects of the concentration of competitive ions to the P removal abilities of LDH, LDH/PMA, and LDH/PMA/BC. (d) Changes in the P-adsorption capacity of LDH/PMA/BC with respect to the adsorption time. (e) Changes in the adsorption capacity of LDH/PMA/BC with respect to the initial concentration of P and the temperature. (f) Changes in the zeta potentials of LDH, LDH/PMA, and LDH/PMA/BC with respect to the pH.

PMDA in LDH/PMA/BC$_4$, LDH/PMA/BC, LDH/PMA/BC$_3$, LDH/PMA/BC$_2$, and LDH/PMA/BC$_1$ were 0.1:1, 0.125:1, 0.17:1, 0.33:1, and 0.5:1, respectively. When the amount of BC added increased from 0.1 to 0.125 g, the adsorption capacity of LDH/PMA/BC increased. However, when the amount of BC increased from 0.125 to 0.5 g, the adsorption capacity of LDH/PMA/BC decreased. Therefore, the optimal amount of BC was 0.125 g. The effect of the amount of BC added on the adsorption capacity of LDH/PMA/BC was analysed. When the amount of BC added increased from 0.1 to 0.125 g, the specific surface area and porosity of LDH/PMA/BC increased, resulting in an increase in the number of exposed functional groups (such as carboxyl groups) in LDH/PMA/BC, which increased the adsorption capacity of LDH/PMA/BC. However, when the amount of BC increased from 0.125 to 0.5 g, the proportion of PMA in LDH/PMA/BC decreased, reducing the content of carboxyl groups in LDH/PMA/BC and thus reducing the adsorption capacity of LDH/PMA/BC.

The adsorption capacities of LDH, LDH/PMA, and LDH/PMA/BC at different pH values also studied (Fig. 5a). As shown in Fig. 5a, in the range of pH 3–8, the adsorption capacity of LDH/PMA was approximately twice that of LDH, indicating that PMA significantly improves

the ability of LDH to adsorb P. Notably, when the pH of the solution was 7, the adsorption capacity of LDH/PMA still reached 69.3 mg g^{-1}, confirming that LDH/PMA is effective for adsorbing P in wastewater. When LDH/PMA was doped with BC, the maximum adsorption capacity of LDH/PMA increased from 76 to 86 mg g^{-1}. This confirmed that BC can slightly improve the adsorption capacity of LDH/PMA for P. However, our control experiments indicated that BC does not have the ability to adsorb P. We examined the BET, FTIR, and XPS results to determine why BC slightly improved the adsorption capacity of LDH/PMA. We found that the addition of BC did not significantly alter the functional groups of LDH/PMA but significantly increased the specific surface area and pore volume of LDH/PMA. Therefore, BC increased the number of functional groups exposed on LDH/PMA that could adsorb P, slightly increasing the adsorption capacity of LDH/PMA.

To investigate the role of PMA in improving the selectivity of LDH to P, the abilities of LDH, LDH/PMA, LDH/PMA/BC to remove P in solutions containing low concentrations of P and high concentrations of competitive ions were evaluated. As shown in Fig. 5c, when the molar ratio of P to coexisting ions increased from 1:0 (0.0002 mol/L:0) to 1:100 (0.0002 mol/L:0.02 mol/L), the rate of P removal by LDH decreased from the initial 100 % to 44 %. However, in the case where PMA was intercalated into LDH, even when the molar concentration ratio of P to coexisting ions increased from 1:0 (0.0002 mol/L:0) to 1:100 (0.0002 mol/L:0.02 mol/L), the rate of P removal by LDH/PMA remained unchanged. The P removal rate was not affected by high concentrations of coexisting ions, indicating high selectivity towards P. Similar to LDH/PMA, LDH/PMA/BC exhibited high selectivity for P. Therefore, PMA plays an important role in improving the P selectivity of LDH/PMA/BC.

3.3. Effect of pH on adsorption capacity of LDH/PMA/BC

The effect of the pH of the solution on the adsorption capacity of LDH/PMA/BC is shown in Fig. 5a. LDH/PMA/BC maintained a significant P adsorption capacity in the range of pH 4–6 (85.5 ± 0.6 mg g^{-1}, 84.6 ± 1.0 mg g^{-1}, and 84.1 ± 0.9 mg g^{-1}). Furthermore, even when the pH of the solution decreased to 3 or increased to 7, the capacity of LDH/PMA/BC to adsorb P only slightly decreased to 72.7 ± 1.0 mg g^{-1} and 74.5 ± 1.0 mg g^{-1}, respectively, indicating that LDH/PMA/BC can effectively adsorb P in a wide pH range (pH 3–7).

To investigate the reason for the effect of the solution pH on the ability of LDH/PMA/BC to adsorb P, we measured the point of zero charge of the adsorbent (Fig. 5f). The point of zero charge (pH_{pzc}) values of LDH, LDH/PMA, and LDH/PMA/BC were 3.2, 3.5, and 3.5, respectively, indicating that LDH, LDH/PMA, and LDH/PMA/BC can adsorb P through electrostatic action only at a pH of < 3. When the pH is > 4, its surface charges are negative, and electrostatic adsorption is not the adsorption mechanism. Although electrostatic adsorption decreased and disappeared with an increase in pH of the solution (pH ≥ 3), the amount of P adsorbed by LDH/PMA/BC exhibited an increasing trend (pH 3–5). This is because PMA contains four carboxyl functional groups (–COOH), and the acidity coefficients of the four carboxyl functional groups are 1.92, 2.87, 4.49, and 5.63. With an increase in the pH of the solution, the four carboxyl groups (–COOH) can deprotonate and become negatively charged esters ($–COO^-$), which can remove P by forming hydrogen bonds with it ($H_2PO_4^-$ and HPO_4^{2-}). However, when the pH of the solution increased from 6, the adsorption capacity of LDH/PMA/BC for P decreased. The reason for this decrease was that the pka^2 of phosphoric acid is 7.2 [27]. Therefore, after the pH increases from 6 to 7.2, the primary form of P changes from $H_2PO_4^-$ to HPO_4^{2-} [28]. $H_2PO_4^-$ has two hydrogen-bond donor groups and one hydrogen-bond acceptor group, whereas HPO_4^{2-} has only one hydrogen-bond donor group and two hydrogen-bond acceptor groups [17]. Therefore, an increase in the number of hydrogen-bond receptor groups on HPO_4^{2-} increases the repulsion between HPO_4^{2-} and the hydrogen-bond receptor groups on LDH/PMA/BC, reducing the amount of P adsorbed by LDH/PMA/BC.

3.4. Kinetic study on adsorption of P by LDH/PMA/BC

We investigated the relationship between the adsorption rate of LDH/PMA/BC and the initial concentration of the P solution (Fig. 5d). For an initial P concentration of 100 mg/L, the adsorption capacity of LDH/PMA/BC for P reached 56 % of its maximum adsorption capacity in the initial 5 min. When the adsorption time was 2 h, the amount of P adsorbed by LDH/PMA/BC reached 85 % of its maximum adsorption capacity. The final adsorption equilibrium was reached in 22 h. For an initial P concentration of 20 mg/L, the adsorption rate of LDH/PMA/BC on P was relatively low. During the initial 5 min and 2 h of contact with the P solution, the adsorption capacity of LDH/PMA/BC only reached 18 % and 55 %, respectively, of its maximum adsorption capacity; however, the final adsorption equilibrium of LDH/PMA/BC for P was reached in 22 h. To further investigate the adsorption mechanism of P on LDH/PMA/BC, the experimental data were fit by pseudo-first- and pseudo-second-order models (Equations 3 and 4).

The parameters fitted by the kinetic model are presented in Table 1. The equilibrium adsorption capacity fitted by the pseudo-first-order model differed from that obtained in the experiment. However, the equilibrium adsorption capacity fitted by the pseudo-second-order model was close to the experimental value, and the R^2 was higher, indicating that chemical adsorption controls the adsorption of P on LDH/PMA/BC [29,30].

3.5. Adsorption isothermal study

The effects of the temperature and initial concentration of the P solution on the adsorption capacity of LDH were investigated. As shown in Fig. 5e, the adsorption capacity of LDH/PMA/BC for P increased with the temperature and initial P concentration. The maximum adsorption capacity of LDH/PMA/BC for P at 10, 25, and 40 °C was 76.9, 97.1, and 108.0 mg g^{-1}, respectively; thus, LDH/PMA/BC had a remarkable adsorption capacity.

To further study the adsorption mechanism of LDH/PMA/BC for P, we examined the isotherm adsorption curve (Fig. 5a) and fitted the adsorption data with the Langmuir equation (Equation 5) [19] and the Freundlich equation (Equation 6). The parameters fitted through the Langmuir and Freundlich isotherm models are presented in Table 2. The R^2 values obtained by the two models were > 0.98; however, the R^2 obtained by the Langmuir isotherm model was slightly higher than that obtained by the Freundlich isotherm model, indicating that monolayer adsorption dominates the process of P adsorption [31,32]. Moreover, the value of 1/n obtained by the Freundlich isotherm model was < 1, indicating that the adsorption of P by LDH/PMA/BC is mainly chemical adsorption [33]. According to the Langmuir isotherm model, the maximum adsorption capacities of LDH/PMA/BC for P at 10, 25, and 40 °C are 80, 99, and 109.9 mg P/g, respectively. Compared with the maximum adsorption capacities of P on lanthanum hydroxide and lanthanum carbonate adsorbent previously reported by us (71.9 mg g^{-1}) [7], La-based porous polyacrylonitrile nanofibers (50.4 mg g^{-1}) [34], an MgO-functionalised cellulose sponge (28.3 mg g^{-1}) [35], and calcium aluminate decahydrate (89.6 mg g^{-1}) [10], LDH/PMA/BC based on hydrogen bonding is advantageous for P adsorption. In addition,

Table 1
Kinetics of P adsorption on LDH/PMA/BC.

$C_{initial}$ (mg/L)	q_e^{exp} (mg/g)	Pseudo-first order model			Pseudo-second order model		
		k_1 (min^{-1})	q_e^{cal} (mg/g)	R^2	k_2 (g $mg^{-1}min^{-1}$)	q_e^{cal} (mg/g)	R^2
20	36.7	2.1×10^{-3}	25.7	0.95	2.5×10^{-4}	38.2	0.99
100	66.4	2.8×10^{-3}	20.5	0.80	6.3×10^{-4}	67.6	0.99

Table 2
P adsorption data of LDH/PMA/BC at different temperatures.

	Langmuir isotherm model			Freundlich isotherm model		
T (°C)	q_m (mg g^{-1})	K_L (L mg^{-1})	R^2	K_F (L mg^{-1})	1/n	R^2
10	80.0	9.1×10^{-2}	0.99	3.7	0.25	0.99
25	99.0	9.6×10^{-2}	0.98	4.0	0.27	0.97
40	109.9	10.2×10^{-2}	0.98	4.3	0.46	0.97

compared with previously reported LDHs [36], the most significant advantage of LDH/PMA/BC is its high selectivity for P, and even when the concentration of competitive ions is 100 times that of P, the removal efficiency of LDH/PMA/BC for P is not affected by competitive ions.

3.6. Effect of coexisting ions on selectivity of LDH/PMA/BC to P

The anions that often coexist with P in wastewater are Cl^-, NO_3^-, SO_4^{2-}, and HCO_3^-. These competitive ions are classified as hydrogen-bond acceptors (Cl^-, NO_3^-, and SO_4^{2-}) and hydrogen-bond donors (HCO_3^-). The effects of the concentration of coexisting ions on the removal rate and selectivity of LDH/PMA/BC for P were investigated (Fig. 7).

3.6.1. Effect of competitive ions of hydrogen-bond acceptor

Because wastewater containing P is generally weakly acidic or weakly alkaline, we investigated the effects of hydrogen-bond acceptor competitive ions (Cl^-, NO_3^-, and SO_4^{2-}) on the removal rate and selectivity of LDH/PMA/BC for P at pH values of 6 and 8 (Fig. 6a and 6b, respectively). As shown in Fig. 6a and 6b, regardless of whether the pH of the solution was 6 or 8, even when the molar concentration of hydrogen-bond acceptor competitive ions (Cl^-, NO_3^-, and SO_4^{2-}) was 10 times that of P, the removal rate of P by LDH/PMA/BC was not affected. This confirms that LDH/PMA/BC has a strong anti-interference ability based on hydrogen bonding for removing P.

However, the concentration of hydrogen-bond acceptor competitive ions can affect the selectivity of LDH/PMA/BC to P. Specifically, when the pH was 6 and the molar ratios of P to competitive ions were 1:1 and 1:5 (mol:mol), the selectivity of LDH/PMA/BC to P was 97.3 % and 94.1 %, respectively. When the molar concentration ratio of LDH/PMA/BC increased to 1:10 (mol:mol), the selectivity of LDH/PMA/BC to P decreased to 73 %. The reduction in the selectivity is attributed to LDH/PMA/BC adsorbing P and SO_4^{2-}. Although the presence of a high concentration of SO_4^{2-} reduce the selectivity of LDH/PMA/BC to P, according to the calculation of the initial molar amounts of P and SO_4^{2-} in the solution, the adsorbed P accounted for 89 % of its initial molar amount, whereas the adsorbed SO_4^{2-} accounted for only 3.3 % of its initial molar amount. This indicates that LDH/PMA/BC has a highly selective adsorption capacity for P. When the pH of the solution was 8 and the molar ratios of P to competitive ions were 1:1 and 1:5, the selectivity of LDH/PMA/BC to P was 100 %. When the molar ratio of P to competitive ions increased to 1:10, the selectivity to P decreased to 78 %.

When a high concentration of hydrogen-bond acceptor-type competitive ions coexists with P (1:10, mol:mol), the removal rate of P by LDH/PMA/BC is unaffected by the competitive ions; however, the selectivity of LDH/PMA/BC to P is slightly reduced. The reasons for this phenomenon are explained below. LDH/PMA/BC adsorbs P by forming hydrogen bonds with the carboxyl groups on its surface. The hydrogen-bond acceptor-type competitive ions cannot form hydrogen bonds with

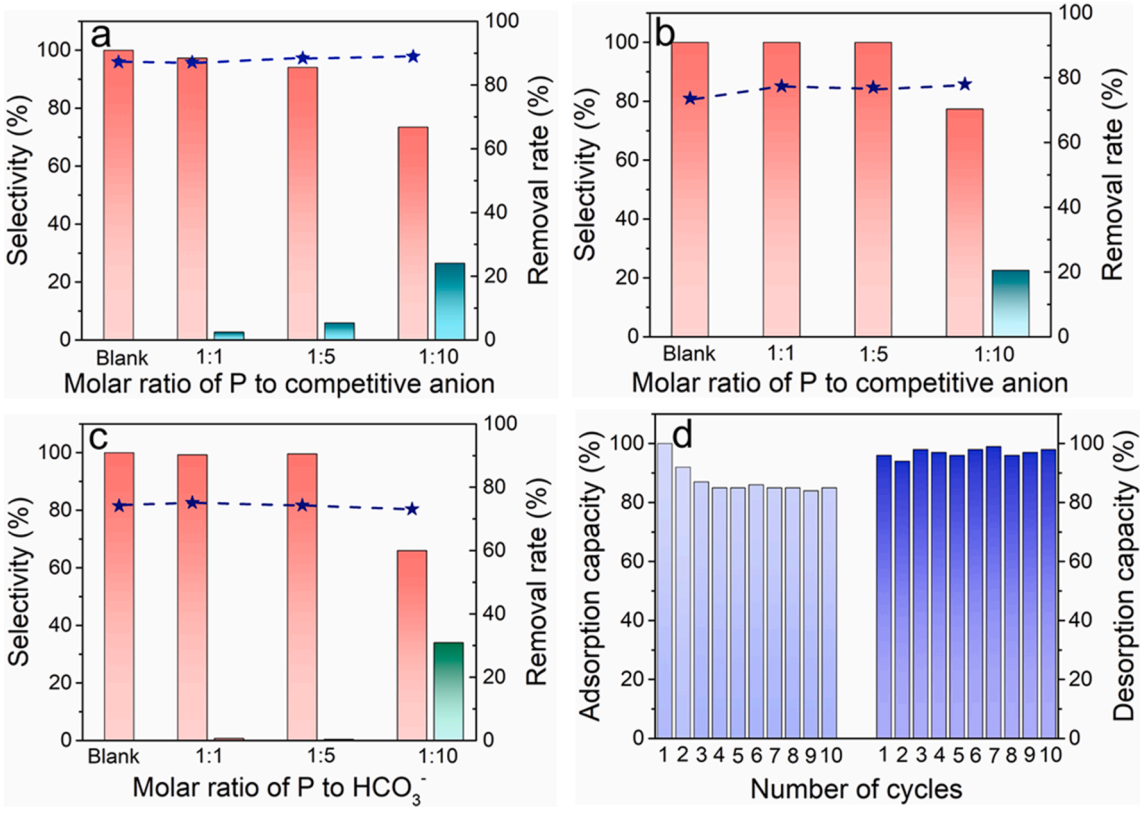

Fig. 6. (a) Effects of the hydrogen-bond acceptor ion concentration on the selectivity and removal rate of LDH/PMA/BC for P at a pH of 6. (b) Effects of the hydrogen-bond acceptor ion concentration on the selectivity and removal rate of LDH/PMA/BC for P at a pH of 8. (c) Effects of the HCO_3^- concentration on the selectivity and removal rate of LDH/PMA/BC for P (the bar chart represents the selectivity for P, and the line represents the removal rate of P). (The red and green bar charts respectively represent the selectivity of LDH/PMA/BC towards P and towards all competing ions. The dotted line represents the remove rate of LDH/PMA/BC to P). (d) Ability of LDH/PMA/BC to adsorb and desorb P in 10 adsorption–desorption cycles. (For interpretation of the references to colour in this figure legend, the reader is referred to the web version of this article.)

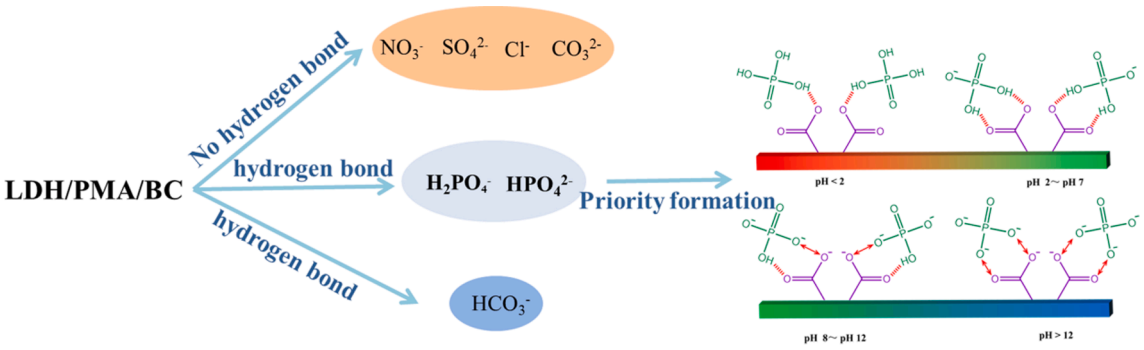

Fig. 7. Selective adsorption mechanism of LDH/PMA/BC for P.

the carboxyl groups on LDH/PMA/BC, because they do not contain H. Therefore, regardless of the concentration of the hydrogen-bond acceptor-type competitive ions, they cannot compete with P for hydrogen-bonding sites; thus, they do not affect the P removal ability of LDH/PMA/BC. However, in this study, the selectivity of LDH/PMA/BC to P was calculated according to the ratio of the molar amount of P adsorbed on LDH/PMA/BC to the total molar amount of anions adsorbed on LDH/PMA/BC, i.e. $R = n_1/(n_1 + n_2) \times 100\ \%$, where n_1 represents the molar amount of P adsorbed, and n_2 represents the molar amount of competitive ions adsorbed. The hydrogen-bond acceptor-type competitive ions cannot compete with P for the hydrogen-bonding adsorption sites on LDH; therefore, they do not affect the value of n_1. However, when the concentration of competing ions is high, a small portion of competing ions form the inner sphere complex with Zn/Al on LDH/PMA/BC through ligand exchange, increasing n_2, which reduces the selectivity of LDH to P.

3.6.2. *Effect of competitive ions of hydrogen-bond donor type*

HCO_3^- is a competitive ion that often coexists with P and functions as a hydrogen-bond donor in wastewater. Theoretically, HCO_3^- and P ($H_2PO_4^-$ and HPO_4^{2-}) can react as hydrogen-bond donors with hydrogen-bond acceptor groups on LDH/PMA/BC to form hydrogen bonds; however, the competitive relationship between HCO_3^- and P remains unclear. Nonetheless, this competitive relationship determines the selectivity of the adsorbent to P based on hydrogen bonding. Therefore, we analysed the selective adsorption capacity of LDH/PMA/BC for P ($H_2PO_4^-$ and HPO_4^{2-}) and HCO_3^- under different concentrations and clarified the competitive relationship between them. HCO_3^- can ionise to form CO_3^{2-} ions in an aqueous solution; therefore, its existing forms in an aqueous solution depend on the pH of the solution. At a pH of 8, it primarily exists in the form of HCO_3^-. Therefore, to study the competition between HCO_3^- and P, we conducted the adsorption experiment at a pH of 8 (Fig. 6c).

The results of the adsorption experiment indicated that the presence of HCO_3^- did not affect the adsorption capacity of LDH/PMA/BC for P. Even when the molar concentration of HCO_3^- was 10 times that of P, the adsorption capacity of LDH/PMA/BC for P was not affected. However, the selectivity of LDH/PMA/BC to P was affected by HCO_3^-. When the molar ratios of P to HCO_3^- were 1:1 and 1:5, the selectivity of LDH/PMA/BC to P was still as high as 99.3 % and 99.6 %, respectively. However, when the molar ratio of P to HCO_3^- increased to 1:10, the selectivity of LDH/PMA/BC to P decreased to 66 %. Although the selectivity to P decreased, LDH/PMA/BC adsorbed 89 % of the initial molar amount of P and only 4.6 % of the initial molar amount of HCO_3^-. In conclusion, LDH/PMA/BC has a strong anti-interference and selective adsorption ability for P in a specific concentration range of competitive ions.

A high concentration of HCO_3^- did not affect the rate of P removal by LDH/PMA/BC but affected the selectivity of LDH/PMA/BC to P, possibly because the carboxyl groups on LDH/PMA/BC, as hydrogen-bond acceptors, preferentially formed hydrogen bonds with P. When LDH/PMA/BC reached its maximum adsorption capacity for P, its carboxyl groups, as adsorption sites, still had not reached saturation, and the unsaturated carboxyl groups (adsorption sites) reacted with a small amount of HCO_3^- to form hydrogen bonds. Therefore, the P removal rate of LDH/PMA/BC was not affected by high concentrations of HCO_3^-, but its selectivity to P decreased owing to the high concentrations of HCO_3^-.

3.7. *Regeneration ability of LDH/PMA/BC and ability to recover P*

The world is facing the double dilemma of the eutrophication of water bodies and the imminent depletion of phosphate rock resources. Using a highly selective adsorbent to remove and recover P from wastewater is an effective way to resolve this dilemma. The regeneration capacity of the adsorbent determines the cost of its application, and its P recovery capacity determines its application potential for the recovery of P resources.

In this study, we conducted 10 adsorption–desorption cycles (Fig. 6d). The results indicated that although there was a slight downward trend in the adsorption capacity of LDH/PMA/BC, the adsorption capacity remained stable after the fifth adsorption cycle. At the 10th cycle, LDH/PMA/BC retained 85 % of its initial P adsorption capacity. The results of the regeneration experiment indicated that LDH/PMA/BC has an excellent regeneration adsorption capacity and is economically feasible for practical applications. In addition, we studied the ability of LDH/PMA/BC to recover P by calculating the P content in the desorption solution. LDH/PMA/BC recovered > 95 % of adsorbed P in 10 cycles, confirming its potential to remove and recover P.

3.8. *Adsorption mechanism of LDH, LDH/PMA and LDH/PMA/BC for P*

The zeta potential, XPS, and FTIR results were analysed to investigate the mechanism of P adsorption by LDH, LDH/PMA, and LDH/PMA/BC (Fig. 7). The points of zero charge value for LDH, LDH/PMA, and LDH/PMA/BC are 3.2, 3.5 and 3.5, respectively. Therefore, when the pH of the P solution is 6 or 8, the LDH, LDH/PMA, and LDH/PMA/BC surfaces are negatively charged, which indicates that P adsorption by LDH, LDH/PMA, and LDH/PMA/BC does not occur via physical electrostatic adsorption.

The FTIR results indicated that LDH exhibits a peak corresponding to P = O at 1032.4 cm^{-1} after adsorbing P. After LDH adsorbs P and coexisting ions, the peak corresponding to P = O at 1032.4 cm^{-1} shifts to 1022.2 cm^{-1}, and a new peak corresponding to adsorbed coexisting anions appears at 1109.5 cm^{-1}, indicating that LDH can not only adsorb P but also coexisting ions, with low selectivity for P. In addition, the peak corresponding to the stretching vibration of the –OH group in LDH shifted from 3458.1 cm^{-1} to 3448.9 cm^{-1}. This shows that the –OH group participated in the adsorption of P, indicating that LDH mainly adsorbed P through ligand exchanges, which is consistent with the XPS results. The XPS results indicated that after the adsorption of P/coexisting ions, the peaks corresponding to Zn 2p, Al 2p, and O 1 s on LDH show significant shifts. The significant shift of these three peaks is due to

ligand exchange between P and –OH on LDH, which leads to the formation of inner spherical complexes of P and Zn/Al on LDH [26]. In addition, another adsorption mechanism of LDH is that the ion exchange between interlayer ions of LDH and P/coexisting ions.

For LDH/PMA and LDH/PMA/BC, the FTIR results show that whether it is only adsorbing P or adsorbing P and competing ions, peaks corresponding to P = O were observed at 1033.5 cm^{-1} on the surfaces of LDH/PMA and LDH/PMA/BC, and no new peaks corresponding to adsorbed coexisting ions were observed. This phenomenon indicates that LDH/PMA and LDH/PMA/BC selectively adsorb P, even in the presence of coexisting ions. This result confirms that the mechanism of adsorption by LDH/PMA and LDH/PMA/BC is different from that of LDH. The mechanism of adsorption by LDH/PMA and LDH/PMA/BC was confirmed by the FTIR and XPS results. The FTIR results showed that after the adsorption of P/coexisting ions, the peaks corresponding to carboxyl groups in LDH/PMA and LDH/PMA/BC shifted significantly, indicating that carboxyl groups participated in the adsorption of P through hydrogen bonding. This FTIR result is consistent with the XPS result. The XPS results for LDH/PMA and LDH/PMA/BC showed the shift in the peaks corresponding to Zn 2p, Al 2p was not significant, which indicates that the ligand exchange between –OH and P was minimal. Therefore, the above results demonstrate that LDH adsorbs P primarily through ligand exchange between –OH and P, whereas LDH/PMA and LDH/PMA/BC adsorb P primarily through hydrogen bonding between COO– and P.

4. Conclusions

We synthesised carboxylated biochar to selectively adsorb P from water for solving the problem of P removal and recovery from sewage. LDH/PMA/BC, which is based on hydrogen bonds, can distinguish the P and competing ions of the hydrogen-bond acceptors (Cl^-, NO_3^-, and SO_4^{2-}) and the P and competing ions of the hydrogen-bond donor (HCO_3^-). In addition, it has an excellent regenerative adsorption capacity and the potential to recover high-purity P. This study provides a useful technical method for the selective removal and recovery of P.

CRediT authorship contribution statement

Yimin Huang: Conceptualization, Investigation, Funding acquisition, Data curation, Writing – original draft. **Dafeng Zhang:** Investigation. **Hongguang Cheng:** Resources, Funding acquisition, Writing – review & editing. **Yingnan He:** Investigation. **Guangzhi Hu:** Writing – review & editing, Project administration, Supervision.

Declaration of Competing Interest

The authors declare that they have no known competing financial interests or personal relationships that could have appeared to influence the work reported in this paper.

Data availability

Data will be made available on request.

Acknowledgments

This work was financially supported by the State Key Laboratory of Environmental Geochemistry (SKLEG2022216), Postdoctoral Research Projects Funding of Yunnan Province (C615300504015), and Double First Class University Construction Project (C176220100042).

Appendix A. Supplementary data

Supplementary data to this article can be found online at https://doi.org/10.1016/j.seppur.2023.125159.

Appendix C. Supplementary data

Supplementary data to this article can be found online at https://doi.org/10.1016/j.seppur.2023.125159.

References

[1] H. Bacelo, A.M.A. Pintor, S.C.R. Santos, R.A.R. Boaventura, C.M.S. Botelho, Performance and prospects of different adsorbents for phosphorus uptake and recovery from water, Chemical Engineering Journal 381 (2020), 122566, https://doi.org/10.1016/j.cej.2019.122566.
[2] Q. Yu, Y. Zheng, Y. Wang, L. Shen, H. Wang, Y. Zheng, N. He, Q. Li, Highly selective adsorption of phosphate by pyromellitic acid intercalated ZnAl-LDHs: Assembling hydrogen bond acceptor sites, Chemical Engineering Journal 260 (2015) 809–817, https://doi.org/10.1016/j.cej.2014.09.059.
[3] Vikrant, Kumar, Kim, Ki-Hyun, Ok, Yong, Sik, Tsang, Daniel, W. C., Engineered/designer biochar for the removal of phosphate in water and wastewater, Science of the Total Environment (2018) 1242-1260. 10.1016/j.scitotenv.2017.10.193.
[4] X. Yu, Y. Nakamura, M. Otsuka, D. Omori, S. Haruta, Development of a novel phosphorus recovery system using incinerated sewage sludge ash (ISSA) and phosphorus-selective adsorbent, Waste Management 120 (2021) 41–49, https://doi.org/10.1016/j.wasman.2020.11.017.
[5] Y. Abdellaoui, H. Abou Oualid, A. Hsini, B. El Ibrahimi, M. Laabd, M. El Ouardi, G. Giácoman-Vallejos, P. Gamero-Melo, Synthesis of zirconium-modified Merlinoite from fly ash for enhanced removal of phosphate in aqueous medium: Experimental studies supported by Monte Carlo/SA simulations, Chemical Engineering Journal 404 (2021), 126600, https://doi.org/10.1016/j.cej.2020.126600.
[6] M. Du, Y. Zhang, Z. Wang, M. Lv, A. Tang, Y. Yu, X. Qu, Z. Chen, Q. Wen, A. Li, Insight into the synthesis and adsorption mechanism of adsorbents for efficient phosphate removal: Exploration from synthesis to modification, Chemical Engineering Journal 442 (2022), 136147, https://doi.org/10.1016/j.cej.2022.136147.
[7] Y. Huang, Y. He, H. Zhang, H. Wang, W. Li, Y. Li, J. Xu, B. Wang, G. Hu, Selective adsorption behavior and mechanism of phosphate in water by different lanthanum modified biochar, Journal of Environmental Chemical Engineering 10 (3) (2022), 107476, https://doi.org/10.1016/j.jece.2022.107476.
[8] D. Luo, L. Wang, H. Nan, Y. Cao, H. Wang, T.V. Kumar, C. Wang, Phosphorus adsorption by functionalized biochar: a review, Environmental Chemistry Letters (2022), https://doi.org/10.1007/s10311-022-01519-5.
[9] Y. Huang, X. Lee, M. Grattieri, M. Yuan, R. Cai, F.C. Macazo, S.D. Minteer, Modified biochar for phosphate adsorption in environmentally relevant conditions, Chemical Engineering Journal 380 (2020), 122375, https://doi.org/10.1016/j.cej.2019.122375.
[10] P. Cheng, Y. Liu, L. Yang, Q. Ren, X. Wang, Y. Chi, H. Yuan, S. Wang, Y.-X. Ren, Phosphate adsorption using calcium aluminate decahydrate to achieve low phosphate concentrations: Batch and fixed-bed column studies, Journal of Environmental Chemical Engineering 11 (2) (2023), 109377, https://doi.org/10.1016/j.jece.2023.109377.
[11] P.S. Kumar, L. Korving, M.C.M. van Loosdrecht, G.-J. Witkamp, Adsorption as a technology to achieve ultra-low concentrations of phosphate: Research gaps and economic analysis, Water Research X 4 (2019), 100029, https://doi.org/10.1016/j.wroa.2019.100029.
[12] B. Wu, J. Wan, Y. Zhang, B. Pan, I.M.C. Lo, Selective Phosphate Removal from Water and Wastewater using Sorption: Process Fundamentals and Removal Mechanisms, Environmental Science and Technology 54 (1) (2020) 50–66, https://doi.org/10.1021/acs.est.9b05569.
[13] Y. Hu, Y. Du, G. Nie, T. Zhu, L. Zhang, Selective and efficient sequestration of phosphate from waters using reusable nano-Zr(IV) oxide impregnated agricultural residue anion exchanger, The Science of the Total Environment 700 (2019), 134999, https://doi.org/10.1016/j.scitotenv.2019.134999.
[14] Z. Wang, D. Shen, F. Shen, T. Li, Phosphate adsorption on lanthanum loaded biochar, Chemosphere 150 (2016) 1–7, https://doi.org/10.1016/j.chemosphere.2016.02.004.
[15] Y. Tardy, P. Vieillard, Relationships among Gibbs free energies and enthalpies of formation of phosphates, oxides and aqueous ions, Contributions to Mineralogy and Petrology 63 (1) (1977) 75–88.
[16] D. Chen, H. Yu, M. Pan, B. Pan, Hydrogen bonding-orientated selectivity of phosphate adsorption by imine-functionalized adsorbent, Chemical Engineering Journal 433 (2022), 133690, https://doi.org/10.1016/j.cej.2021.133690.
[17] B. Saha, S. Chakraborty, G. Das, A mechanistic insight into enhanced and selective phosphate adsorption on a coated carboxylated surface, Journal of Colloid and Interface Science 331 (1) (2009) 21–26, https://doi.org/10.1016/j.jcis.2008.11.007.
[18] S.-N. Zhuo, T.-C. Dai, H.-Y. Ren, B.-F. Liu, Simultaneous adsorption of phosphate and tetracycline by calcium modified corn stover biochar: Performance and mechanism, Bioresource Technology 359 (2022), 127477, https://doi.org/10.1016/j.biortech.2022.127477.
[19] T. Van Truong, Y.-J. Kim, D.-J. Kim, Study of biochar impregnated with Al recovered from water sludge for phosphate adsorption/desorption, Journal of Cleaner Production 383 (2023), 135507, https://doi.org/10.1016/j.jclepro.2022.135507.
[20] S. Yang, Q. Wang, H. Zhao, D. Liu, Bottom-up synthesis of MOF-derived magnetic Fe-Ce bimetal oxide with ultrahigh phosphate adsorption performance, Chemical

Engineering Journal 448 (2022), 137627, https://doi.org/10.1016/j.cej.2022.137627.
[21] P.R. Rout, P. Bhunia, R.R. Dash, Effective utilization of a sponge iron industry by-product for phosphate removal from aqueous solution: A statistical and kinetic modelling approach, Journal of the Taiwan Institute of Chemical Engineers 46 (2015) 98–108, https://doi.org/10.1016/j.jtice.2014.09.006.
[22] J. Huo, X. Min, Q. Dong, S. Xu, Y. Wang, Comparison of Zn–Al and Mg–Al layered double hydroxides for adsorption of perfluorooctanoic acid, Chemosphere 287 (2022), 132297, https://doi.org/10.1016/j.chemosphere.2021.132297.
[23] L. Yang, Q. Wang, H. Yao, Q. Yang, X. Lu, Z. Wu, R. Liu, K. Shi, S. Ma, The confinement effect of layered double hydroxides on intercalated pyromellitic acidic anions and highly selective uranium extraction from simulated seawater, Dalton Transactions 51 (21) (2022) 8327–8339, https://doi.org/10.1039/D2DT01278B.
[24] Y. Cao, G. Shen, Y. Zhang, C. Gao, Y. Li, P. Zhang, W. Xiao, L. Han, Impacts of carbonization temperature on the Pb(II) adsorption by wheat straw-derived biochar and related mechanism, The Science of the Total Environment 692 (2019) 479–489, https://doi.org/10.1016/j.scitotenv.2019.07.102.
[25] S. Lee, J. Choi, K. Song, K. Choi, Y. Lee, K. Jung, Adsorption and mechanistic study for phosphate removal by rice husk-derived biochar functionalized with Mg/Al-calcined layered double hydroxides via co-pyrolysis, Composites Part B: Engineering 176 (2019) 107209, https://doi.org/10.1016/j.compositesb.2019.107209.
[26] H. Zhang, Q. Wang, J. Zhang, G. Chen, Z. Wang, Z. Wu, Development of novel ZnZr-COOH/CNT composite electrode for selectively removing phosphate by capacitive deionization, Chemical Engineering Journal 439 (2022), 135527, https://doi.org/10.1016/j.cej.2022.135527.
[27] B.K. Mahata, S.-M. Chang, P. Bose, Bio-Inspired phosphate adsorption by Copper-Decorated weak base anion exchanger, Separation and Purification Technology 296 (2022), 121339, https://doi.org/10.1016/j.seppur.2022.121339.
[28] M. Du, Y. Zhang, Z. Wang, M. Lv, Q. Xu, Z. Chen, Q. Wen, A. Li, La-doped activated carbon as high-efficiency phosphorus adsorbent: DFT exploration of the adsorption mechanism, Separation and Purification Technology 298 (2022), 121585, https://doi.org/10.1016/j.seppur.2022.121585.
[29] W.-X. Liang, Y. Wei, M. Qiao, J.-W. Fu, J.-X. Wang, High-gravity-assisted controlled synthesis of lanthanum carbonate for highly-efficient adsorption of phosphate, Separation and Purification Technology 307 (2023), 122696, https://doi.org/10.1016/j.seppur.2022.122696.
[30] Z. Lan, Y. Lin, C. Yang, Lanthanum-iron incorporated chitosan beads for adsorption of phosphate and cadmium from aqueous solutions, Chemical Engineering Journal 448 (2022), 137519, https://doi.org/10.1016/j.cej.2022.137519.
[31] G. Cai, Z.-L. Ye, Concentration-dependent adsorption behaviors and mechanisms for ammonium and phosphate removal by optimized Mg-impregnated biochar, Journal of Cleaner Production 349 (2022), 131453, https://doi.org/10.1016/j.jclepro.2022.131453.
[32] X. Hong, S. Zhu, M. Xia, P. Du, F. Wang, Investigation of the efficient adsorption performance and adsorption mechanism of 3D composite structure La nanosphere-coated Mn/Fe layered double hydrotalcite on phosphate, Journal of Colloid and Interface Science 614 (2022) 478–488, https://doi.org/10.1016/j.jcis.2022.01.149.
[33] W.-J. Xia, L.-X. Guo, L.-Q. Yu, Q. Zhang, J.-R. Xiong, X.-Y. Zhu, X.-C. Wang, B.-C. Huang, R.-C. Jin, Phosphorus removal from diluted wastewaters using a La/C nanocomposite-doped membrane with adsorption-filtration dual functions, Chemical Engineering Journal 405 (2021), 126924, https://doi.org/10.1016/j.cej.2020.126924.
[34] X. Jia, H. Wang, Y. Li, J. Xu, H. Cheng, M. Li, S. Zhang, H. Zhang, G. Hu, Separable lanthanum-based porous PAN nanofiber membrane for effective aqueous phosphate removal, Chemical Engineering Journal 433 (2022), 133538, https://doi.org/10.1016/j.cej.2021.133538.
[35] Y. Cheng, Q. Xie, Z. Wu, L. Ji, Y. Li, Y. Cai, P. Jiang, B. Yu, Mechanistic insights into the selective adsorption of phosphorus from wastewater by MgO(100)-functionalized cellulose sponge, The Science of the Total Environment 868 (2023), 161646, https://doi.org/10.1016/j.scitotenv.2023.161646.
[36] K.-H. Goh, T.-T. Lim, Z. Dong, Application of layered double hydroxides for removal of oxyanions: A review, Water Research 42 (6) (2008) 1343–1368, https://doi.org/10.1016/j.watres.2007.10.043.